

Estimation of Crustal Deformation and Magnitude of the 2011 off the Pacific coast of Tohoku Earthquake Using Strong Ground Motion Records

T. Hirai & N. Fukuwa

Nagoya University, Nagoya, Japan



SUMMARY

The 2011 off the Pacific coast of Tohoku Earthquake (M_w 9.0) is the greatest earthquake in Japan. Analysis of GPS network, such as GEONET by Geospatial Information Authority of Japan, has revealed the crustal deformation distribution due to the earthquake. On the other hand, the permanent displacement due to the earthquake can be estimated from the displacement waveform, which is calculated by integrating the acceleration waveform observed by strong ground motion seismograph. This method could be used complementary with GPS analysis. In this study, we calculated the permanent displacement distribution due to the 2011 off the Pacific coast of Tohoku Earthquake and estimated its moment magnitude using relation between permanent displacements and hypocentre distances. The result suggests that quick estimation of unsaturated magnitude can be realized by calculating displacement waveforms using strong ground motion records at extremely large earthquake.

Keywords: Crustal deformation, Strong motion record, 2011 off the Pacific coast of Tohoku Earthquake

1. INTRODUCTION

In plate subduction zones, large interplate earthquakes occur repeatedly on the interface between subducting oceanic and overriding continental plates. An interplate earthquake occurs when the shear stress on the plate interface caused by plate subduction reaches its frictional strength. Japan trench, which lies off the eastern coast of Tohoku district of Japan, is one of such plate subduction zones. The 2011 off the Pacific coast of Tohoku Earthquake (M_w 9.0) occurred on March 11, 2011, in this area. It is the greatest earthquake in Japan. The first report of JMA (Japan Meteorological Agency) magnitude estimated at 3 minutes after initiation was 7.9. Furthermore, the moment magnitude which should be calculated at about 15 minutes after initiation was not calculated due to the saturation of broadband seismographs. As a result, the tsunami height was underestimated resulting in loss of many lives unfortunately. Now southwest Japan faces the hazard of great earthquake of Suruga and Nankai trough, which lies off the Pacific coast of southwest Japan. It is extremely important to construct the quick estimation system of unsaturated magnitude, such as moment magnitude defined by Hanks and Kanamori (1979).

Systematic difference between JMA and moment magnitude for extremely large earthquake have discussed conventionally (e.g. Utsu, 2001). JMA magnitude is calculated based on the peak velocity or displacement of strong ground motion records, whose component is until 5 s period. Since JMA magnitude can be calculated about 3 minutes after the earthquake, it is very useful to announce tsunami alert quickly. However, signal level of objective period range is saturated for over M 8 earthquake and calculated JMA magnitude saturates for such earthquake. On the other hand, since tsunami height depends on the amount of coseismic crustal deformation of seafloor mainly, the moment magnitude reflecting the amount of fault slip should be used for tsunami alert system essentially, instead of JMA magnitude.

Attenuation relation between intensity of seismic motion and hypocentre distance can be used to estimate magnitude of an earthquake. For example, Si and Midorikawa (1999) proposed the empirical

relation between peak velocity or acceleration and distance from seismic fault, in which moment magnitude of the earthquake is included as a parameter. But this relation is determined from seismic records due to under M 8.3 earthquakes. Katsumata *et al.* (2011) proposed the empirical relation between peak displacement and hypocentre distance using the seismograms of a lot of earthquakes including the 2011 off the Pacific coast of Tohoku Earthquake, in which moment magnitude is included as a parameter, too. Hirai and Fukuwa (2011) pointed out the possibility of quick estimation of moment magnitude using relation between coseismic displacements and hypocentre distances. Above reports suggests that moment magnitude can be estimated by plotting the amounts of seismic motion or displacement versus distances from seismic source. Since moment magnitude nearly agrees with JMA magnitude in under about M 8 earthquake, present method to estimate JMA magnitude is well useful. For larger earthquakes, another method which uses long-period component of seismic motion effectively is required.

In this study, we first explain the procedure to calculate coseismic displacement using strong ground motion record and next develop the method to estimate moment magnitude of the earthquake using relation between coseismic displacements and hypocentre distances. Then we evaluate our method applying it to the 2011 off the Pacific coast of Tohoku Earthquake and future great earthquake of Suruga and Nankai Trough.

2. THEORY

2.1. Calculation of coseismic displacement

Time series of acceleration is defined as second order derivative of that of displacement. So that once an acceleration record is given, corresponding displacement waveform can be calculated by integrating it. Permanent displacement is the final value of the displacement waveform. We integrate acceleration records using linear acceleration method as follows:

$$v_i = \begin{cases} 0 & (i = 0) \\ v_{i-1} + \frac{a_i + a_{i-1}}{2} \Delta t & (i \geq 1) \end{cases} \text{ and} \quad (2.1)$$

$$d_i = \begin{cases} 0 & (i = 0) \\ d_{i-1} + v_{i-1} \Delta t + \left(\frac{a_{i-1}}{3} + \frac{a_i}{6} \right) \Delta t^2 & (i \geq 1) \end{cases}, \quad (2.2)$$

where Δt denotes the sampling period, a_i , v_i , and d_i denote acceleration, velocity, and displacement at time $i\Delta t$, respectively. Using Eqn (2.1) and Eqn (2.2), digital acceleration record can be integrated to digital velocity and displacement waveform. However, acceleration waveform recorded by servo sensor often changes its baseline discontinuously one or more times during the record (Boore 2001; Aoi *et al.*, 2009). Calculated displacement waveform diverges to infinity in this case. Therefore, observed acceleration record should be corrected by some procedures. In this study, we use following two correction procedures to get realistic displacement waveform.

At first, discontinuous change of acceleration baseline appears as a bend of velocity waveform. Constant slope of velocity waveform came from constant acceleration which is not zero. Hence integrating acceleration waveform and fitting it to two straight lines,

$$y(t; t_c, m) = U(t - t_c) m (t - t_c), \quad (2.3)$$

where m and t_c are parameters, $U(t)$ denotes unit step function. Subtracting derivative of Eqn (2.3) from original acceleration record, the corrected acceleration waveform is derived. Parameters m and t_c is determined by minimizing sum of residual error between velocity waveform and Eqn (2.3),

$$P(t_c, m) = \int_0^T [v(t) - y(t; t_c, m)]^2 dt, \quad (2.4)$$

where T denotes the duration time of acceleration record. Corrected acceleration waveform can be calculated by following equation:

$$a^*(t) = a(t) - \frac{dy(t; t_c, m)}{dt} = a(t) - mU(t - t_c) \quad (2.5)$$

Second, an acceleration waveform sometimes has many slight baseline changes in its duration. To correct these baseline changes, original acceleration record should be integrated and fitted to polygonal line. But its procedure is very complex and unsuitable to correct many acceleration records automatically. Boore *et al.* (2002) suggested that fitting velocity waveform to a quadratic curve is useful to correct slight baseline changes in many cases. This method is formulized as

$$y(t; p, q) = U(t - t_a) [p(t^2 - t_a^2) + q(t - t_a)], \quad (2.6)$$

where t_a denotes the arrival time of seismic wave. Parameters p and q are determined by minimizing sum of residual error between velocity waveform and Eqn (2.6)

$$P(p, q) = \int_0^T [v(t) - y(t; p, q)]^2 dt. \quad (2.7)$$

Corrected acceleration waveform can be calculated by following equation:

$$a^*(t) = a(t) - \frac{dy(t; p, q)}{dt} = a(t) - U(t - t_a)(2pt + q) \quad (2.8)$$

Once realistic displacement waveform is calculated, permanent displacement is defined as the final value of the displacement.

2.2. Convergence ratio

An example of displacement waveform is shown in Fig. 2.1. For convenience, we define convergence ratio of displacement waveform by following equation:

$$\text{convergence ratio} = 1 - h/H, \quad (2.9)$$

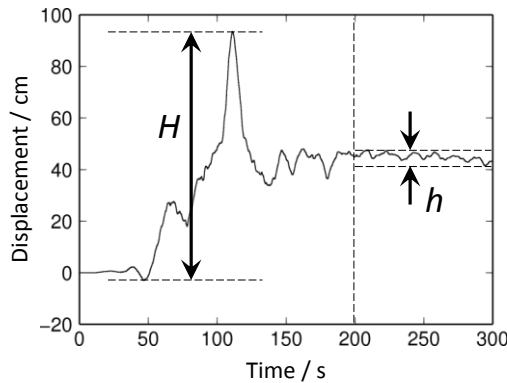


Figure 2.1. Example of displacement waveform

where h and H are defined in Fig. 2.1. Small value of convergence ratio means good and stable estimation of permanent displacement.

2.3. Estimation of moment magnitude

Applying the theory of elasticity, seismic moment, and then moment magnitude, of the earthquake can be estimated using the relation between permanent displacements and hypocentre distances. For infinite linear elastic medium, relation between displacement at arbitrary point $u_i(t)$ due to a point source and hypocentre distance is represented as follows:

$$\begin{aligned}
u_i(t) = & \sum_{p=1}^3 \sum_{q=1}^3 \left[\frac{A_{ipq}^N}{4\pi\rho R^4} \int_{R/\alpha}^{R/\beta} s M_{pq}(t-s) ds \right. \\
& + \frac{A_{ipq}^{IP}}{4\pi\rho\alpha^2 R^2} M_{pq} \left(t - \frac{R}{\alpha} \right) + \frac{A_{ipq}^{IS}}{4\pi\rho\beta^2 R^2} M_{pq} \left(t - \frac{R}{\beta} \right) \\
& \left. + \frac{A_{ipq}^{FP}}{4\pi\rho\alpha^3 R} \dot{M}_{pq} \left(t - \frac{R}{\alpha} \right) + \frac{A_{ipq}^{FS}}{4\pi\rho\beta^3 R} \dot{M}_{pq} \left(t - \frac{R}{\beta} \right) \right], \quad (2.10)
\end{aligned}$$

where ρ , α , and β denote density, P-wave velocity, and S-wave velocity respectively, A_{ipq} is direction coefficient, $M_{pq}(t)$ is time series of moment tensor. The fourth and fifth terms do not contribute to permanent displacement because they are proportional to the time derivative of moment tensor. Considering the limit of infinite time on Eqn (2.10), the permanent displacement U_i is given as

$$U_i = \psi_i M_0 / 4\pi\mu R^2 \quad (2.11)$$

with

$$\psi_i = \sum_{p=1}^3 \sum_{q=1}^3 \left[\frac{1}{2} \left(1 - \frac{\beta^2}{\alpha^2} \right) A_{ipq}^N + \frac{\beta^2}{\alpha^2} A_{ipq}^{IP} + A_{ipq}^{IS} \right] (n_p v_q + n_q v_p), \quad (2.12)$$

where μ denotes shear modulus. To derive Eqn (2.12), representation of moment tensor in the case of fault slip

$$M_{pq} = (n_p v_q + n_q v_p) M_0 \quad (2.13)$$

is used, where n_i and v_i denote i -component of unit normal vector of the fault and unit slip direction vector respectively, M_0 denotes the seismic moment. According to Eqn (2.11), permanent displacement is in proportion to the seismic moment and is inverse proportion to square of the hypocentre distance. Permanent displacement is, however, influenced by the direction effect. In this study, we use the concise formula including average of direction coefficient and surface effect coefficient $f_s = 2$,

$$U = f_s \Phi M_0 / 4\pi\mu R^2 \quad (2.14)$$

with

$$\Phi = \frac{1}{4\pi} \int_0^{2\pi} \int_0^\pi \sqrt{\psi_1^2 + \psi_2^2 + \psi_3^2} \sin\theta d\theta d\varphi. \quad (2.15)$$

Taking logarithm of each side of Eqn (2.13), we obtain

$$\log U = -2\log R + \log(f_s \Phi M_0 / 4\pi\mu). \quad (2.16)$$

According to Eqn (2.16), the seismic moment, and then moment magnitude, is given in the form of the intercept of straight line of slope -2 plotting the permanent displacements versus hypocentre distances on double logarithmic chart.

3. DATA

We use the acceleration records due to the 2011 off the Pacific coast of Tohoku Earthquake recorded on the strong ground motion observation network K-NET and KiK-net by National Research Institute for Earth Science and Disaster Prevention, Japan. Each KiK-net station exists at more rigid site than K-NET stations and has strong ground motion seismographs both surface and bedrock levels. As a comparison of permanent displacement, we refer the coseismic displacement distribution revealed by ARIA team at JPL and Caltech (2011), which is based on observation of Global Positioning System (GPS) network GEONET by Geospatial Information Authority, Japan. We assume that shear modulus and Poisson ratio of crust are $\mu = 40$ GPa and $\nu = 0.25$, respectively. Average direction coefficient is calculated as $\Phi = 0.63$ in this condition.

4. RESULT FOR THE 2011 OFF THE PACIFIC COAST OF TOHOKU EARTHQUAKE

4.1. Coseismic displacement distribution

In this study, two procedures of baseline correction are applied. At first, Fig. 4.1 shows an example of the first correction procedure. The acceleration record is east-west component observed at surface of KiK-net FKSH09 station. Fig. 4.1 (a), (b) and (c) represent original acceleration, velocity and displacement waveform, while (d), (e) and (f) represent corrected acceleration, velocity and displacement waveform, respectively. According to Fig. 4.1, the original velocity waveform has one bending point at 120 s from recording start, so we found that the original acceleration waveform has one discontinuous baseline change at 120 s from recording start. The velocity derived from corrected acceleration has no bending point, consequently corrected displacement waveform does not diverge and permanent displacement converges to finite value stably. Second, Fig. 4.2 shows an example of the second correction procedure. The acceleration record is east-west component observed at bedrock of KiK-net AKTH10 station. Fig. 4.2 (a), (b) and (c) represent original acceleration, velocity and displacement waveform, while (d), (e) and (f) represent corrected acceleration, velocity and displacement waveform, respectively. Although the original velocity waveform has no evident bending, displacement waveform does not converge to constant value. But the corrected displacement waveform converges to constant value.

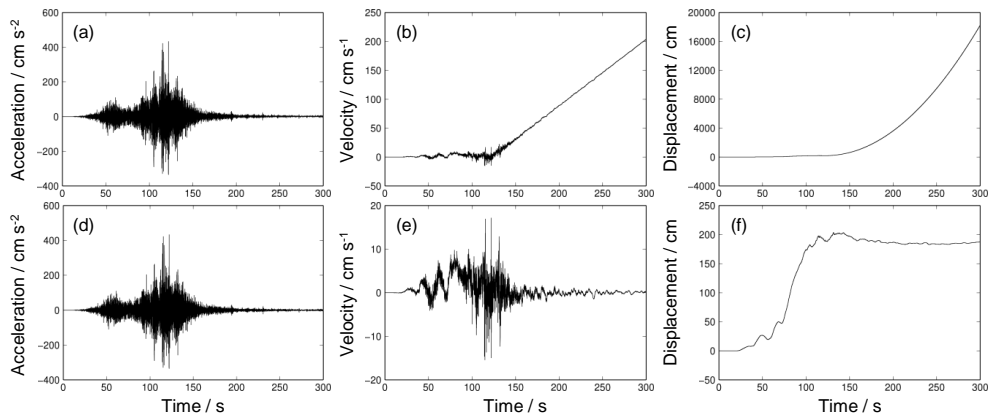


Figure 4.1. Example of the first procedure of baseline correction

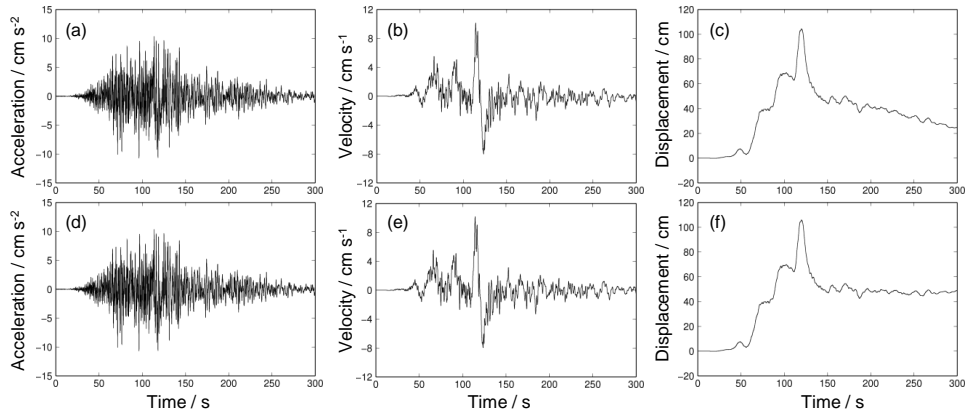


Figure 4.2. Example of the second procedure of baseline correction

Due to the 2011 off the Pacific coast of Tohoku Earthquake, huge crustal deformation occurred in Tohoku district, Japan. Crustal deformation distribution is obtained as permanent displacement of each station. Fig. 4.3 shows distribution of permanent displacement calculated from acceleration records and coseismic displacements observed by GPS network GEONET.

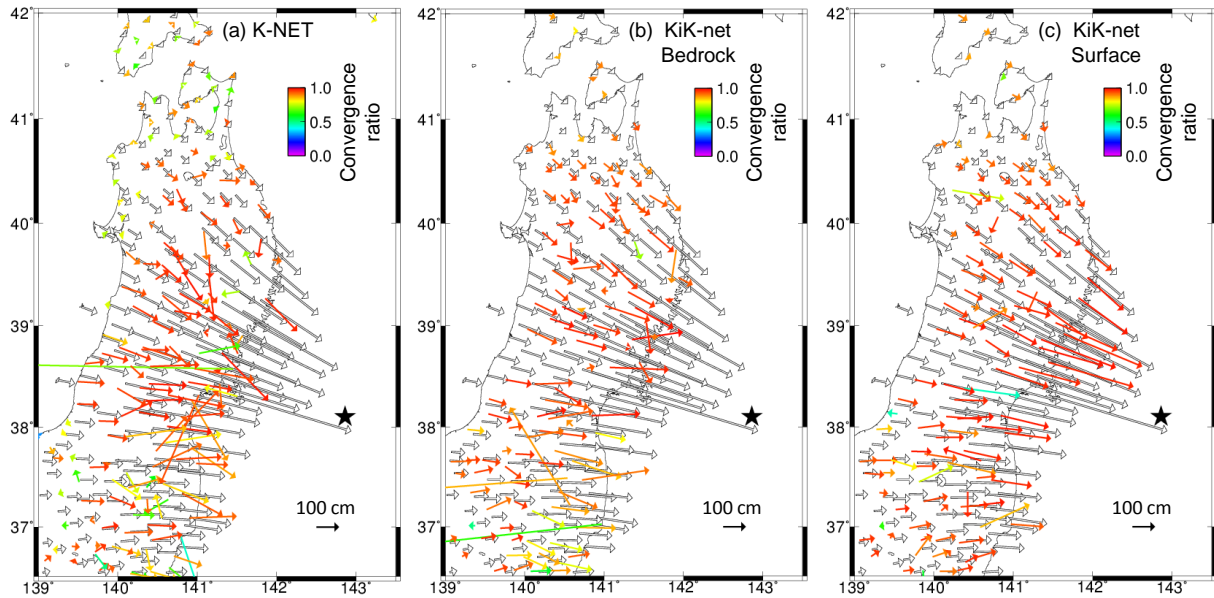


Figure 4.3. Permanent displacement distribution due to the 2011 off the Pacific coast of Tohoku Earthquake

In Fig. 4.3, coloured vectors represent permanent displacements calculated from acceleration records, white vectors represent coseismic displacements observed by GPS network. Colour of vectors corresponds to the convergence ratio defined as Eqn (2.9). Black star represents the epicentre of the 2011 off the Pacific coast of Tohoku Earthquake. According to Fig. 4.3, the result for KiK-net bedrock is more stable than results for K-NET and KiK-net surface. Such difference reflects soil condition of the station. As mentioned in Section 3, most of KiK-net stations exist on more rigid site than K-NET stations. In addition, since each KiK-net station has two seismographs at its surface and bedrock level, the latter can record ground acceleration without amplification effect of soil. Therefore, acceleration records on bedrock of KiK-net stations are most suitable for estimating coseismic displacement distribution.

4.2. Estimation of moment magnitude

Applying the theory of elasticity, the moment magnitude can be estimated using the relation between

coseismic displacements and hypocentre distances. In this study, we apply Eqn (2.16) to not only permanent displacements but also temporal displacements assuming that short-period component is enough smaller than long-period component in displacement waveform. Fig. 4.4 shows the result for estimation of moment magnitude of the 2011 off the Pacific coast of Tohoku Earthquake. Each panel in Fig. 4.4 represents 15 s, 30 s, 45 s, 1 min, 2 min, 3 min, 4 min, 5 min, 10 min and 15 min after rupture initiation, respectively. All solid lines in Fig. 4.4 are drawn with slope -2, so that moment magnitude is estimated for each panel as the intercepts of the lines. According to Fig. 4.4, the moment magnitude of the 2011 off the Pacific coast of Tohoku Earthquake is estimated as $M_w = 8.9$ finally. The result is consistent with source process analysis based on coseismic crustal deformation observed by GPS network (e.g. Ito *et al.*, 2011). The estimated moment magnitude increases with time reflecting the propagation of fault rupture. For example, Ide *et al.* (2011) revealed that the fault rupture finished about 2 minutes after rupture initiation. The time until estimated moment magnitude becomes stable corresponds to rupture continuation and seismic wave propagation.

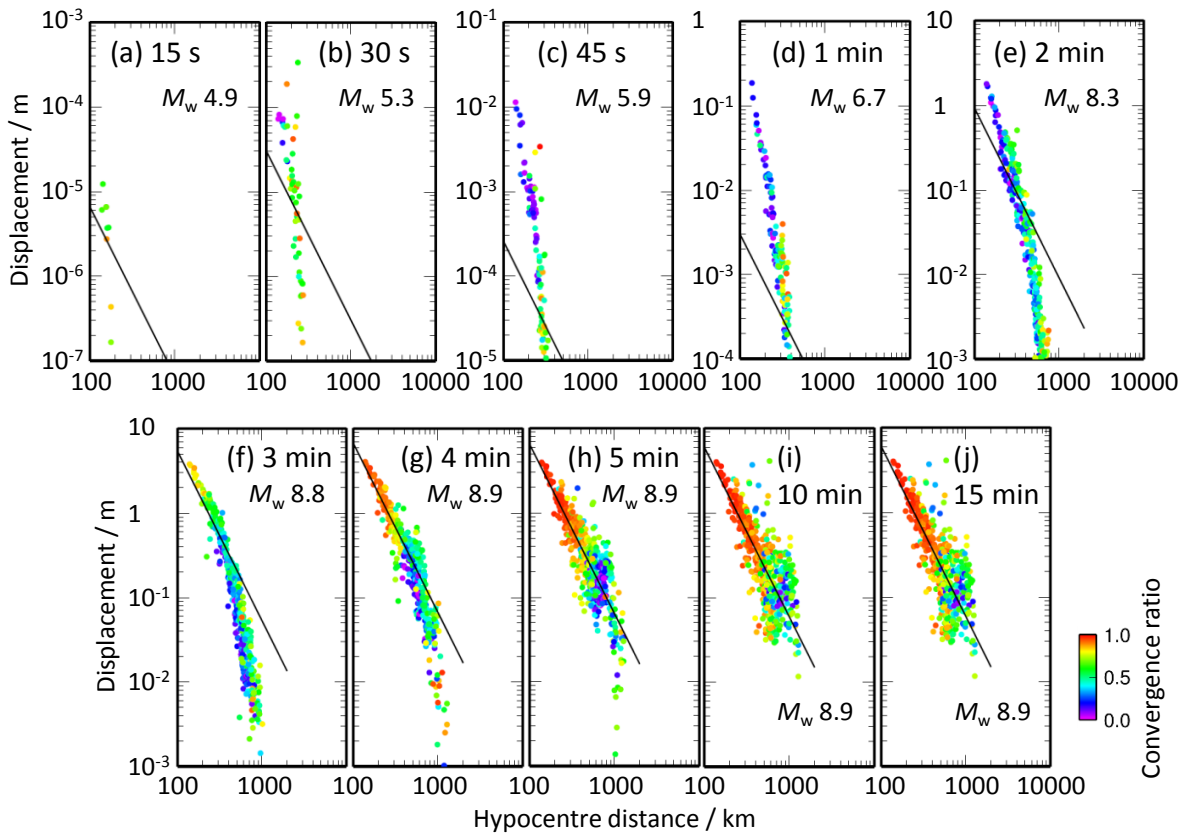


Figure 4.4. Real time estimation of moment magnitude for the 2011 off the Pacific coast of Tohoku Earthquake

5. APPLICATION TO FUTURE SURUGA AND NANKAI TROUGH EARTHQUAKE

Philippine Sea plate is subducting under Eurasian plate at off the Pacific coast of southwest Japan, which trench is called Suruga and Nankai Trough. Now it is afraid that three great interplate earthquakes, named Tokai, Tonankai and Nankai earthquake, would occur coincidentally in this area in future several decades. Total magnitude is assumed to be 8.7 for damage estimation.

In this section, we apply our moment magnitude estimation method to future great earthquake of Suruga and Nankai Trough. Fig. 5.1 shows the settings of seismogenic faults and displacement observation points. The seismogenic fault model is from Central Disaster Prevention Council, Japan (2003). In Fig. 5.1, grey and white squares denote element faults of asperity and background area, respectively. Opened circles denote displacement observation points, which arrangement is same to that of KiK-net. Black stars are assumed rupture initiation points for two cases: A. off Kii Peninsula

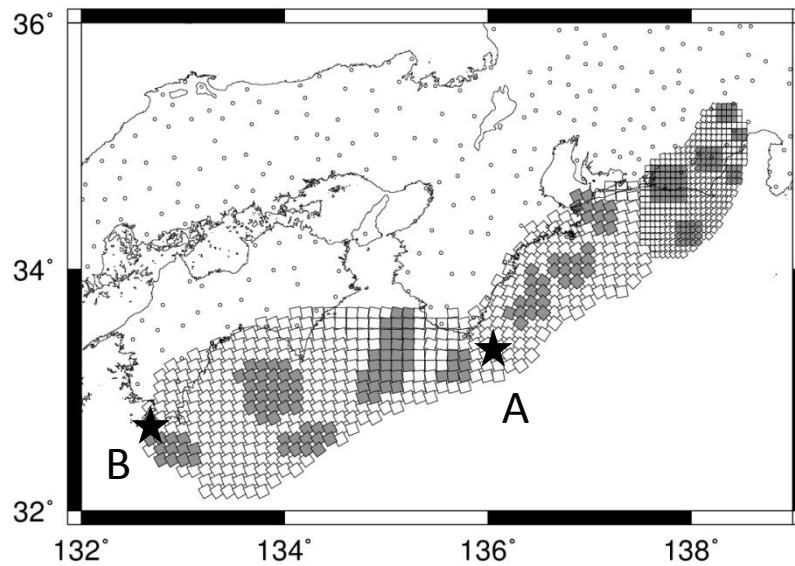


Figure 5.1. Settings of seismogenic faults and displacement observation points for future great earthquake of Suruga and Nankai Trough

and B. off Ashizuri Cape. Since the rupture initiation point of future great earthquake of Suruga and Nankai Trough is not predicted clearly, we assumed two hypocenters as mostly considerable cases. Displacement waveforms due to the earthquake are calculated based on Eqn (2.10) assuming that moment tensor time series is expressed by ramp function. Fig. 5.2 and Fig. 5.3 show the results for real time estimation of moment magnitude of each case. Each panel in Fig. 5.2 and Fig. 5.3 represents 15 s, 30 s, 45 s, 1 min, 2 min, 3 min, 4 min, 5 min, 10 min and 15 min after rupture initiation, respectively. Although estimated moment magnitude increases with time, it saturates in 4 minutes after rupture initiation. Final value of estimated moment magnitude 8.6 is almost consistent with the seismogenic fault model in both cases of rupture initiation point. However, residual errors are very large in the case of rupture initiation at off Ashizuri Cape against its accuracy moment magnitude estimation. This result can be explained as follows: the total moment magnitude 8.7 is contributed by all parts of seismogenic faults. Therefore, at observation point near the hypocentre, displacement is smaller than expected amount by point source with $M_w = 8.7$. On the other hand, at observation point existing far east from hypocentre, displacement is greater than expected amount by point source at hypocentre. The former leads moment magnitude to underestimation, while the latter leads moment magnitude to overestimation. As a result of mixing of these two effects, estimated moment magnitude becomes almost correct. This problem comes from the assumption of point source which is used in moment magnitude estimation method described in Section 2.3. To construct more theoretically rational estimation method, line source assumption or finite fault model should be brought to the scheme. But in immediately following earthquake initiation, it is difficult to know where the fault rupture terminates. Therefore, we brought point source assumption in this study for simplicity. Solution of this problem is expected to be proposed in the future.

6. CONCLUSION

We developed a method to calculate displacement time series and permanent displacement due to an earthquake accurately using acceleration waveform recorded by strong ground motion seismograph in this study. Additionally, we also suggested that moment magnitude of an earthquake can be estimated using the relation between displacements due to the earthquake and hypocentre distances based on the theory of elasticity. Applying our method to the 2011 off the Pacific coast of Tohoku Earthquake, the coseismic displacement distribution was calculated reasonably and the moment magnitude was estimated almost accurately. From the result for real time estimation of moment magnitude, it was found that the moment magnitude increases with time and saturate at $M_w = 8.9$ in 4 minutes after

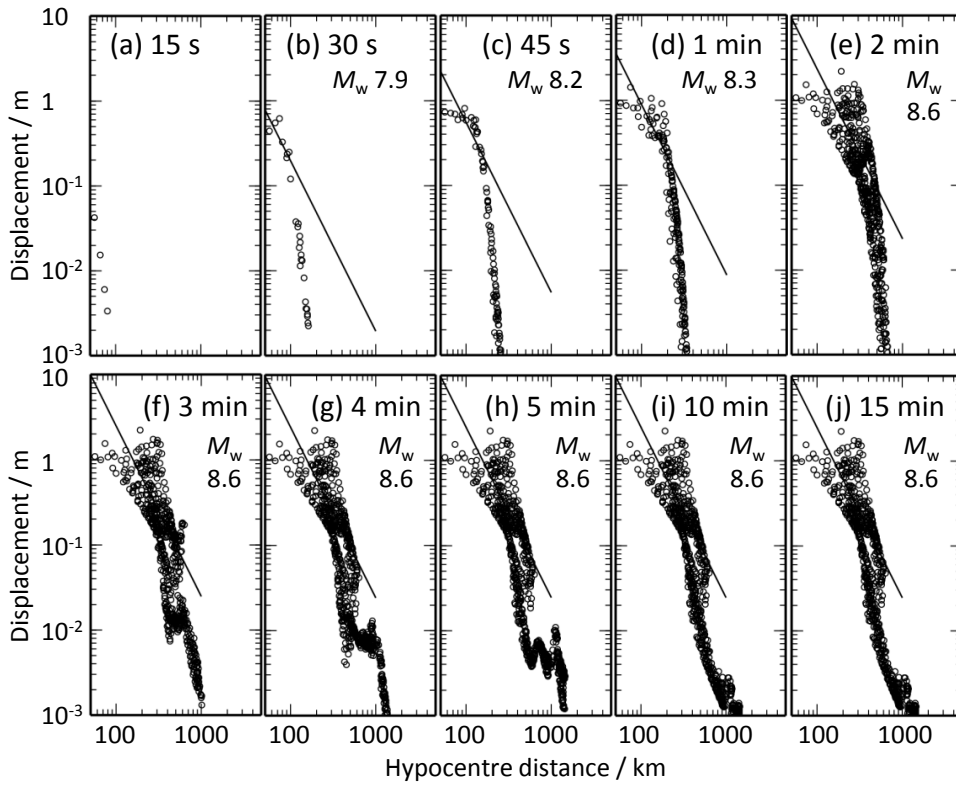


Figure 5.2. Real time estimation of moment magnitude for future Suruga and Nankai Trough earthquake assuming rupture initiation at off Kii Peninsula

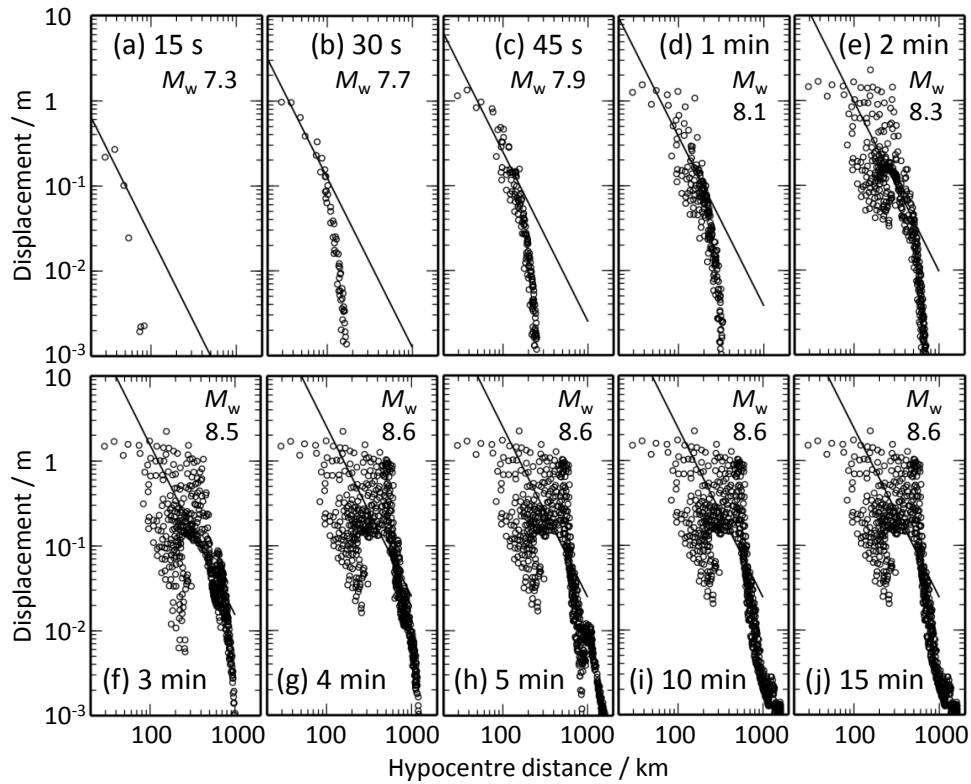


Figure 5.3. Real time estimation of moment magnitude for future Suruga and Nankai Trough earthquake assuming rupture initiation at off Ashizuri Cape

rupture initiation. These estimations of the moment magnitude are consistent with that by source process analysis based on coseismic crustal deformation observed by GPS network. In order to evaluate the validity of our method for future great earthquake of Suruga and Nankai Trough, we synthesised the displacement waveforms due to the earthquake based on the seismic fault model for two cases of rupture initiation point: off Kii Peninsula and off Ashizuri Cape. Applying our method to synthesised displacement waveforms, it is found that the moment magnitude of the earthquake would be estimated almost accurately in 4 minutes after rupture initiation in both cases. Above results suggest that our method would be a powerful tool to estimate coseismic crustal deformation and moment magnitude of an earthquake quickly, so that it can play an important role in long-period seismic motion and tsunami alert system.

ACKNOWLEDGEMENT

We used the acceleration records observed on strong ground motion observation network K-NET and KiK-net by National Research Institute for Earth Science and Disaster Prevention, Japan. We also used the result for GPS analysis on the 2011 off the Pacific coast of Tohoku Earthquake by ARIA team at JPL and Caltech (2011), which data is sourced by Geospatial Information Authority, Japan. Some figures in this paper were prepared using Generic Mapping Tools by Wessel and Smith (1995).

REFERENCES

- Aoi, S., Kunugi, T., Adachi, S. and Fujiwara, H. (2009). Deployment of new strong-motion seismographs of K-NET and KiK-net. *2nd Euro-mediterranean meeting on Accelerometric Data Exchange and Archiving*. ARIA team at JPL and Caltech (2011). <ftp://sideshow.jpl.nasa.gov/pub/usrs/ARIA>.
- Boore, D.M. (2001). Effect of baseline corrections on displacements and response spectra for several recordings of the 1999 Chi-Chi, Taiwan, Earthquake. *Bull. Seismol. Soc. Am.* **91**, 1199-1211.
- Boore, D.M., Stephens, C.D. and Joyner, W.B. (2002). Comments on baseline correction of digital strong-motion data: examples from the 1999 Hector Mine, California, Earthquake. *Bull. Seismol. Soc. Am.* **92**, 1543-1560.
- Central Disaster Prevention Council, Japan (2003). Material No. 3 for 16th expert committee on the Tokai and Tonankai Earthquake (in Japanese).
- Hanks, T.C. and Kanamori, H. (1979). A moment magnitude scale. *J. Geophys. Res.* **84**, 2348-2350.
- Hirai, T. and Fukuwa N. (2011). Estimation of crustal deformation due to the 2011 off the Pacific coast of Tohoku Earthquake based on strong ground motion record and potential for real-time moment magnitude determination. *2011 Fall Meeting, Seismological Society of Japan*, 132 (in Japanese).
- Hirai, T. and Fukuwa, N. (2012). Estimation of crustal deformation distribution due to the 2011 off the Pacific coast of Tohoku Earthquake based on strong motion records. *J. Struct. Constr. Eng., AIJ* **77:673**, 341-350 (in Japanese).
- Ide, S., Baltay, A. and Beroza, G.C. (2011). Shallow dynamic overshoot and energetic deep rupture in the 2011 M_w 9.0 Tohoku-Oki Earthquake. *Science* **332**, 1426-1429.
- Ito, T., Ozawa, K., Watanabe, T. and Sagiya, T. (2011). Slip distribution of the 2011 off the Pacific coast of Tohoku Earthquake inferred from geodetic data. *Earth Planets Space* **63**, 627-630.
- Katsumata, A., Aoki, S., Yoshida, Y. and Kimura, K. (2011). Quick magnitude determination based on peak velocity and displacement. *2011 Fall Meeting, Seismological Society of Japan*, 230 (in Japanese).
- Si, H. and Midorikawa, S. (1999). New attenuation relationships for peak ground acceleration and velocity considering effects of fault type and site condition. *J. Struct. Constr. Eng., AIJ* **523**, 63-70 (in Japanese).
- Utsu, T. (2001), Seismology, Kyoritsu Shuppan Co., Ltd. (in Japanese).
- Wessel, P. and Smith, W.H.F. (1995). New version of the Generic Mapping Tools released. *Eos Trans. AGU* **76**, 329.